

Gap formation in monolayer and bilayer graphene with Coulomb interaction

Andreas Sinner and Klaus Ziegler

Institute for Physics, University of Augsburg, D-86135 Augsburg, Germany

(Dated: February 20, 2019)

We study the gap opening due to the repulsive Coulomb interaction in monolayer and bilayer graphene in the vicinity of the charge neutrality point by employing the functional renormalization-group technique. It is shown that the effect of the Coulomb interaction in both graphene configurations is rather different as a consequence of the different low-energy spectra. The gap formation is always supported in monolayer graphene and guarantees the finiteness of the Fermi velocity. In bilayer graphene the gap is either suppressed or supported, depending on the bare gap parameter. This indicates a metal-insulator transition due to Coulomb interaction. The corresponding renormalization-group flow is characterized by the presence of several fixed points which are quite distinct in the two cases.

PACS numbers: 71.10.-w, 05.10.Cc

Monolayer (ML) and bilayer (BL) graphene are semimetals with an electron and a hole band. Both bands touch each other at two nodes, whereas the low-energy dispersion in the vicinity of these nodes is linear in ML graphene and quadratic in BL graphene. Exactly at the nodes both systems obey a chiral symmetry which reflects the sublattice symmetry of the underlying honeycomb lattice. The sublattice symmetry can be broken, either by adding hydrogen atoms to ML graphene [1] or by a biased gate voltage applied to BL graphene [2]. Then the question is whether or not such a gap is suppressed or supported by the Coulomb interaction. Previous studies have shown that disorder induces random fluctuations of the gap which can suppress the effective gap and allow ML and BL graphene to be a conductor and to have a metal-insulator transition for a sufficiently large average gap [3]. On the other hand, it has been discussed by Juričić et al. that a short-range (Gross-Neveu) electron-electron interaction can dominate the long-range Coulomb interaction, leading eventually to an insulating behavior [4]. In contrast, we will follow subsequently a more direct route to an insulator by assuming a small gap and studying how this is affected by the Coulomb interaction itself. The problem of Coulomb interaction in graphene has been previously studied by employing a perturbative renormalization-group (RG) approach, for clean ML graphene [4, 5, 6, 7, 8, 9] as well as for disordered ML graphene [10, 11, 12]. These studies show clearly a strong renormalization of the Fermi velocity in the clean case and considerable interplay between Coulomb interaction and disorder.

At zero temperature the model for both ML and BL graphene is described by the following Euclidean action

$$\mathcal{S}[\psi^\dagger, \psi] = \mathcal{S}_0[\psi^\dagger, \psi] + \mathcal{S}_I[\rho] = - \int_Q \psi_Q^\dagger [iq_0\sigma_0 + h(q_\mu)] \psi_Q + \frac{g}{2} \int_Q \frac{1}{q} \rho_Q \rho_{-Q}, \quad (1)$$

with the same interaction but different kinetic energy parts. The integrals over the momentum and frequency

$Q = (q_0, \vec{q})$ with the absolute value of the momentum q and zero-temperature Matsubara frequency q_0 read $\int_Q = (2\pi)^{-3} \int dq_0 d^2\vec{q}$ and should be thought of being regularized by means of an UV-cutoff Λ_0 . Note that we require the fermionic densities to be of the Lorenz scalar form, i. e. $\rho_Q = \int_P \psi_P^\dagger \sigma_3 \psi_{P+Q}$.

For ML, the Hamiltonian $h(q_\mu)$ in the non-interacting part of the action reads

$$h(q_\mu) = v(q_1\sigma_1 + q_2\sigma_2), \quad (2a)$$

where $v = \sqrt{3}ta/2$ denotes the bare Fermi velocity and for BL

$$h(q_\mu) = (2\mu)^{-1} [(q_1^2 - q_2^2)\sigma_1 + 2q_1q_2\sigma_2] \quad (2b)$$

with the quasiparticle mass $\mu = 2t_\perp/3t^2a^2$. Here, t is the in-plane hopping amplitude, t_\perp the hopping amplitude between the one-atomic graphite sheets, a denotes the lattice spacing. The microscopic strength of the Coulomb interaction between electrons is given by $g = e^2/(4\epsilon_0\epsilon\hbar)$, where e denotes the elementary charge, ϵ_0 the dielectric constant of the vacuum, and ϵ the relative dielectric constant of the substrate.

Now we map the pure fermionic action Eq. (1) onto the action containing both fermionic and bosonic degrees of freedom by means of the Hubbard-Stratonovich transformation [13],

$$\mathcal{S}_0[\psi^\dagger, \psi] + \mathcal{S}_I[\rho] \rightarrow \mathcal{S}_0[\psi^\dagger, \psi] + \mathcal{S}_0[\phi] + \mathcal{S}_Y[\rho, \phi], \quad (3)$$

where the free bosonic action reads

$$\mathcal{S}_0[\phi] = \frac{1}{2g} \int_Q q\phi_Q\phi_{-Q}, \quad (4)$$

and the third term denotes the interacting Yukawa term describing coupling between fermions and bosons:

$$\mathcal{S}_Y[\rho, \phi] = i \int_Q \int_K \psi_K^\dagger \sigma_3 \psi_{K+Q} \phi_{-Q}. \quad (5)$$

If we assume that the scalar bosonic field ϕ has a finite vacuum expectation value, i. e. if we shift it as

$$\phi_Q \rightarrow \hat{\phi}_Q + i\delta_{Q,0}\Delta, \quad (6)$$

then the electronic spectrum of both ML and BL acquires a finite gap, i. e. the Hamiltonian given in Eqs. (2a) and (2b) may be rewritten as $h \rightarrow h + \Delta\sigma_3$. The gap in the fermionic spectrum is thus naturally generated by the symmetry breaking of the bosonic field and causes the violation of the chiral symmetry on the fermionic side.

From the mixed action Eq. (3) we obtain vertices and propagators by taking functional derivatives with respect to each field. From $\delta^2\mathcal{S}/\delta\psi_Q^\dagger\delta\psi_{Q'}|_{\psi^\#, \hat{\phi}=0} = -\delta_{Q,Q'}G_0^{-1}(Q)$, where $\psi^\# = \{\psi^\dagger, \psi\}$, we obtain the inverse fermionic propagator

$$G_0^{-1}(Q) = iq_0\sigma_0 + \Delta\sigma_3 + h(q_\mu), \quad (7a)$$

where we keep $h(q_\mu)$ as defined in Eqs. (2a) and (2b), and from $\delta^2\mathcal{S}/\delta\hat{\phi}_Q\delta\hat{\phi}_{Q'}|_{\psi^\#, \hat{\phi}=0} = -\delta_{Q,Q'}F^{-1}(Q)$ the inverse bosonic propagator.

$$F^{-1}(Q) = -\frac{q}{g}. \quad (7b)$$

Finally, the bare Yukawa vertex is obtained as $\Gamma(P_1; P_2, P_3) = \delta^3\mathcal{S}/\delta\psi_{P_1}^\dagger\delta\psi_{P_2}\delta\hat{\phi}_{P_3}|_{\psi^\#, \hat{\phi}=0}$. We arrive at

$$\Gamma(P_1; P_2, P_3) = i\sigma_3\delta_{P_1, P_2+P_3}. \quad (7c)$$

The functional RG is conveniently defined in terms of the field dependent functional of effective action $\mathcal{L}[\Phi]$, which in turn represents the Legendre transform of the generating functional of connected Green functions. For our purposes the averaged field Φ is supposed to contain both fermionic and bosonic entries [13]. The functional \mathcal{L} depends on the IR-cutoff $\Lambda \leq \Lambda_0$, which is eventually removed. The derivation of the fRG-flow equation is described in detail in [13, 14, 15]. The RG-flow of \mathcal{L} is generated by the regulator function introduced into the propagator of the non-interacting system and is determined by

$$\partial_\Lambda\mathcal{L}_\Lambda[\Phi] = -\frac{1}{2}\text{Tr} \left\{ \partial_\Lambda[G_{0,\Lambda}^R]^{-1} \left(\frac{\delta^2\mathcal{L}_\Lambda^R}{\delta\Phi\delta\Phi}[\Phi] \right)^{-1} \right\}, \quad (8)$$

where $[G_{0,\Lambda}^R]^{-1}$ is the propagator of the non-interacting system containing the regulator function and

$$\left. \frac{\delta^2\mathcal{L}_\Lambda^R}{\delta\Phi\delta\Phi}[\Phi] \right|_{\Phi=0} = -[G_\Lambda^R]^{-1} = -([G_{0,\Lambda}^R]^{-1} - \Sigma_\Lambda) \quad (9)$$

denotes the regularized full inverse propagator with Σ_Λ meaning the irreducible self-energy. The choice of the regulator will be specified a few lines below.

Since our main interest is in the determination of the spectrum renormalization of fermions due to the

Coulomb interaction we will focus on the coupling parameters in the fermionic sector of the theory. In the simplest approximation we make the following ansatz for the running effective action

$$\mathcal{L}_\Lambda[\psi^\dagger, \psi] \approx -\int_Q \psi_Q^\dagger [iq_0\sigma_0 + \Delta_\Lambda\sigma_3 + Z_\Lambda^{-1}h(q_\mu)] \psi_Q, \quad (10)$$

which takes the renormalization of the energy gap and of the electronic dispersion into account. We do not consider the renormalization of the Matsubara frequency since we assume the Coulomb interaction to be absolutely instantaneous. Since for momenta larger than the UV-cutoff Λ_0 the action in Eq. (10) must reproduce the bare fermionic action, the initial conditions are chosen as $Z_{\Lambda_0} = 1$ and $\Delta_{\Lambda_0} = \Delta$.

Taking functional derivatives with respect to the both Grassmanian fields on both sides of Eq. (8) we arrive at the RG-flow equation for the inverse renormalized fermionic propagator. For details of its derivation we refer to Ref. [13]. If we employ the regularization scheme with the regulator built in the fermionic lines only, this equation can be written in the following algebraic form:

$$\partial_\Lambda G_\Lambda^{-1}(Q) = \int_P \sigma_3 \dot{G}_\Lambda(P) \sigma_3 F(P-Q), \quad (11)$$

where $F(Q)$ is the *bare* Coulomb potential defined in Eq. (7b), and the single scale propagator \dot{G}_Λ is defined as

$$\dot{G}_\Lambda = -G_\Lambda^R \partial_\Lambda [G_{0,\Lambda}^R]^{-1} G_\Lambda^R \quad (12)$$

We will work within the so-called sharp cutoff regularization scheme [15]. Then the momentum cutoff is introduced as follows:

$$G_{0,\Lambda}^R(Q) = \Theta(\Lambda < q < \Lambda_0) G_0(Q), \quad (13)$$

where $\Theta(\Lambda < q < \Lambda_0) = \Theta(\Lambda_0 - q) - \Theta(\Lambda - q) \rightarrow \Theta(q - \Lambda)$ as $\Lambda_0 \rightarrow \infty$. For momenta smaller than the UV-cutoff Λ_0 , the flowing fermionic propagator $G_\Lambda^R(Q)$ is

$$G_\Lambda^R(Q) = -\Theta(q - \Lambda) \frac{iq_0\sigma_0 - \Delta_\Lambda\sigma_3 - Z_\Lambda^{-1}h(q_\mu)}{q_0^2 + E_\Lambda^2(q)}, \quad (14)$$

and hence the single-scale propagator [15]

$$\dot{G}_\Lambda(Q) = \delta(q - \Lambda) \frac{iq_0\sigma_0 - \Delta_\Lambda\sigma_3 - Z_\Lambda^{-1}h(q_\mu)}{q_0^2 + E_\Lambda^2(q)}, \quad (15)$$

where we have introduced $E_\Lambda(q) = \sqrt{\Delta_\Lambda^2 + \epsilon_\Lambda^2(q)}$ with the renormalized spectra of free fermions $\epsilon_\Lambda(q) = Z_\Lambda^{-1}vq$ for ML and $\epsilon_\Lambda(q) = (2\mu Z_\Lambda)^{-1}q^2$ for BL. For both ML and BL the flow equations for the coupling parameter Δ_Λ is extracted from Eq. (11) in the same way:

$$\partial_\Lambda\Delta_\Lambda = \frac{1}{2}\text{Tr}_\sigma \{ \sigma_3 \partial_\Lambda G_\Lambda^{-1}(Q) \} \Big|_{Q=0}. \quad (16a)$$

The RG-flow equations for the factor Z_Λ are extracted differently for ML and BL due to the different scaling of spectra in these configurations:

$$\partial_\Lambda Z_\Lambda^{-1} = \frac{1}{2v} \frac{\partial}{\partial q_1} \text{Tr}_\sigma \{ \sigma_1 \partial_\Lambda G_\Lambda^{-1}(Q) \} \Big|_{Q=0}, \text{ ML}, (16b)$$

$$\partial_\Lambda Z_\Lambda^{-1} = \frac{\mu}{2} \frac{\partial^2}{\partial q_1^2} \text{Tr}_\sigma \{ \sigma_1 \partial_\Lambda G_\Lambda^{-1}(Q) \} \Big|_{Q=0}, \text{ BL}. (16c)$$

Introducing the logarithmic flow parameter $\ell = \log(\Lambda_0/\Lambda)$ we obtain

$$\partial_\ell \Delta_\ell = -\frac{1}{4\pi} \frac{g\Delta_\ell \Lambda}{\sqrt{\Delta_\ell^2 + \epsilon_\ell^2}}, \text{ ML and BL}, (17a)$$

$$\partial_\ell Z_\ell = -\frac{1}{8\pi} \frac{gZ_\ell \Lambda}{\sqrt{\Delta_\ell^2 + \epsilon_\ell^2}}, \text{ ML}, (17b)$$

$$\partial_\ell Z_\ell = -\frac{3}{32\pi} \frac{gZ_\ell \Lambda}{\sqrt{\Delta_\ell^2 + \epsilon_\ell^2}}, \text{ BL}, (17c)$$

where we have used the identity $\partial_\ell Z_\ell^{-1} = -Z_\ell^{-2} \partial_\ell Z_\ell$. The flowing free fermion spectra are $\epsilon_\ell = vZ_\ell^{-1}\Lambda$ for ML and $\epsilon_\ell = (2\mu Z_\ell)^{-1}\Lambda^2$ for BL. The scaling dimension of the energy, (i. e. the dynamical exponent) is defined as $z = 1 - \eta_\ell$ for ML and $z = 2 - \eta_\ell$ for BL. Here, η_ℓ is referred to as the anomalous dimension which can be obtained from the parameter Z_ℓ by

$$\eta_\ell = -\partial_\ell \log Z_\ell. (18)$$

In the gapless regime Eqs. (17a)-(17c) are easily solved. The only solution of Eq. (17a) is the trivial one $\Delta_\ell = \Delta_{\ell=0} = 0$, while Eqs. (17b) and (17c) reduce to $\partial_\ell Z_\ell^{-1} = \lambda_{\text{ML}}$ with $\lambda_{\text{ML}} = g/(8\pi v)$ for ML and correspondingly $\partial_\ell Z_\ell^{-1} = \lambda_{\text{BL}} e^\ell$ with $\lambda_{\text{BL}} = 6\mu g/(32\pi\Lambda_0)$ for BL with solutions:

$$Z_\ell^{-1} = 1 + \lambda_{\text{ML}} \ell \text{ for ML}, (19)$$

$$Z_\ell^{-1} = 1 + \lambda_{\text{BL}} (e^\ell - 1) \text{ for BL}. (20)$$

The result of Eq. (19) corresponds to the well-known logarithmic renormalization of the Fermi velocity $v_\ell = Z_\ell^{-1}v$ in clean ML graphene due to the Coulomb interaction [5, 6, 7, 16]. The result of Eq. (20) corresponds to the inverse exponential renormalization of the quasiparticle mass $\mu_\ell = Z_\ell \mu$ in BL. Therefore, the inverse mass diverges as $\ell \rightarrow \infty$. Using Eq. (18) we obtain expressions for the anomalous dimension

$$\eta_\ell = \frac{\lambda_{\text{ML}}}{1 + \lambda_{\text{ML}} \ell} \text{ for ML and} (21a)$$

$$\eta_\ell = \frac{\lambda_{\text{BL}}}{\lambda_{\text{BL}} + (1 - \lambda_{\text{BL}})e^{-\ell}} \text{ for BL}. (21b)$$

For $\ell \rightarrow 0$ Eq. (21a) approaches zero, meaning that the scaling dimension of the energy in ML remains $z = 1$ and nothing changes on the relativistic behavior of electrons.

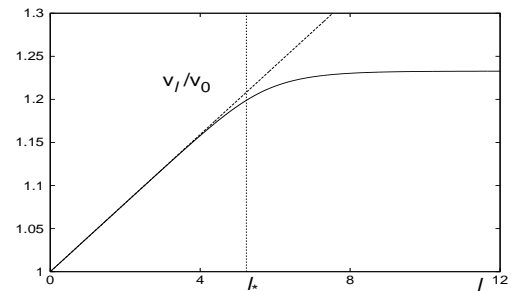


FIG. 1: Renormalization of the Fermi velocity $v_\ell = vZ_\ell^{-1}$ in ML because of Coulomb interaction with (solid line, full solutions of Eqs. (17a) and (17b)) and without a gap (dashed line, Eq. (19)). To the leading order we obtain for the scale $\ell_* \approx -\log(Z_{\ell \rightarrow \infty} \Delta_{\ell \rightarrow \infty} / v\Lambda_0)$.

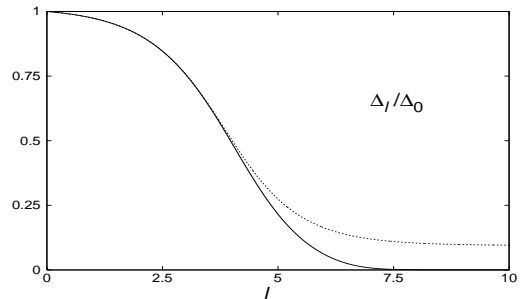


FIG. 2: Flow of the gap parameter Δ_ℓ/Δ_0 in BL. Solid line corresponds to the choice of Δ_0 smaller than some critical value, the dashed line in turn to a starting value larger than the critical one.

In contrast, Eq. (21b) approaches in this limit unity. This means that the scaling dimension of the energy $z = 2 - \eta_\ell$ becomes *relativistic* in BL with the velocity $v_s = 3g/32\pi$, i. e. in vacuum $c/v_s \approx 1450$. Therefore, in absence of a gap in the spectrum of BL the Coulomb interaction attempts to linearize the fermionic dispersion in vicinity of the nodal points.

With a finite starting value for the gap Δ_0 Eqs. (17a)-(17c) cannot be solved exactly anymore but only by iteration. As to ML, the flow of the parameter Δ_ℓ always develops a finite value for $\ell \rightarrow \infty$, no matter how small the initial value is chosen. This corresponds to the opening of the gap in the spectrum that induces an additional scale in ML at which the logarithmic growth of the Fermi velocity stops and it stabilizes at some *finite* value, as depicted in Fig. 1.

In contrast, in BL the flow trajectory of the gap Δ_ℓ crucially depends on the choice of the starting values. If the starting value Δ_0 is chosen to be smaller than some critical value, the gap scales to zero as $\ell \rightarrow \infty$, thus restoring the chiral symmetry of the Hamiltonian and preserving the semimetal character of clean BL. If however the starting value is chosen above the critical value, the flow develops some finite value, i. e. BL changes from a conductor to an insulator, as shown in Fig. 2.

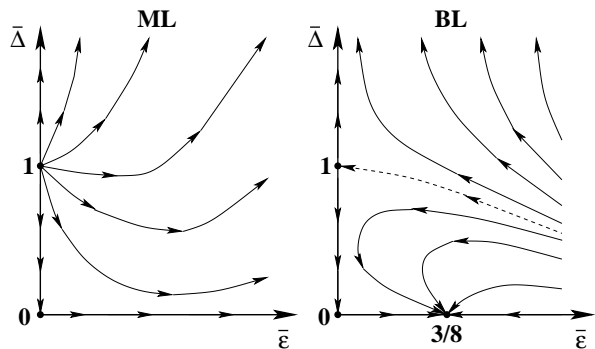


FIG. 3: Schematic RG-flow for both graphene configurations in the space spanned by the dimensionless kinetic energy $\bar{\epsilon}_\ell$ and gap parameter $\bar{\Delta}_\ell$.

In order to shed some light on the topological properties of the RG-flow in the parametric space it is convenient to redefine Eqs. (17b) and (17c) in terms of kinetic energy and introduce dimensionless parameters by expressing both the gap and kinetic energy in units of Coulomb energy: $\bar{\epsilon}_\ell = 4\pi\epsilon_\ell/g\Lambda$ with ϵ_ℓ defined below Eq. (17c) and $\bar{\Delta}_\ell = 4\pi\Delta_\ell/g\Lambda$. We obtain following equations:

$$\partial_\ell \bar{\Delta}_\ell = \bar{\Delta}_\ell - \frac{\bar{\Delta}_\ell}{\sqrt{\bar{\epsilon}_\ell^2 + \bar{\Delta}_\ell^2}}, \quad \text{ML and BL}, \quad (22a)$$

$$\partial_\ell \bar{\epsilon}_\ell = \frac{\bar{\epsilon}_\ell}{2\sqrt{\bar{\epsilon}_\ell^2 + \bar{\Delta}_\ell^2}}, \quad \text{ML}, \quad (22b)$$

$$\partial_\ell \bar{\epsilon}_\ell = -\bar{\epsilon}_\ell + \frac{3\bar{\epsilon}_\ell}{8\sqrt{\bar{\epsilon}_\ell^2 + \bar{\Delta}_\ell^2}}, \quad \text{BL}. \quad (22c)$$

The expression for the anomalous dimension becomes $\eta_\ell = m/\sqrt{\bar{\epsilon}_\ell^2 + \bar{\Delta}_\ell^2}$, with $m = 1/2$ for ML and $m = 3/8$ for BL. The flow in the parametric space is schematically shown in Fig. (3). The fixed points (FPs) are obtained by setting the right-hand sides of Eqs. (22a)-(22c) to zero and solving the emerging system of algebraic equations. For ML there are two FPs at $\bar{\Delta}_* = 1$, $\bar{\epsilon}_* = 0$ and at $\bar{\Delta}_* = 0$, $\bar{\epsilon}_* = 0$. The first FP is totally unstable, i. e. it does not possess any attractive direction. The energy exhibits at this point an anomalous scaling with the anomalous dimension $\eta = 1/2$. No matter in which direction the flow points from this FP it always eventually runs to an infinitely large value of $\bar{\Delta}$ which corresponds to the above mentioned opening of the gap. The only exception is when the flow follows the axis $\bar{\Delta}$ toward the origin of the coordinates. This is the attractive direction of the second quantum FP which corresponds to the infinitely large Coulomb interaction in clean ML which has been predicted by Son in [5]. However, this FP requires a more elaborate treatment due to the strongly increasing scale of λ_{ML} .

The landscape of the parameter space of BL is entirely

different. There are three FPs at $\bar{\Delta}_* = 1$, $\bar{\epsilon}_* = 0$, at $\bar{\Delta}_* = 0$, $\bar{\epsilon}_* = 0$, and at $\bar{\Delta}_* = 0$, $\bar{\epsilon}_* = 3/8$. The main difference with ML is the presence of the separatrix manifold in the plane that corresponds to the critical surface of the metal-insulator transition. This is shown as the dashed line in Fig. 3. Starting below the separatrix line, the flow inevitably runs into the totally attractive FP at $\bar{\Delta}_* = 0$, $\bar{\epsilon}_* = 3/8$ with the anomalous scaling of the energy $\eta = 1$, i. e. with a relativistic spectrum. For each choice of initial conditions above the separatrix the flow runs toward the infinite rescaled gap, i. e. BL becomes an insulator with $\eta = 0$. Finally, moving along the critical surface for which the starting values of parameters have to be adjusted very carefully, the flow ends up in the FP at $\bar{\Delta}_* = 1$, $\bar{\epsilon}_* = 0$. This corresponds to the equally large gap and Coulomb energy with the anomalous dimension $\eta = 3/8$. There is also a fixed point at $\bar{\Delta}_* = 0$, $\bar{\epsilon}_* = 0$, corresponding to the infinitely large Coulomb repulsion.

In conclusion, we have studied both ML and BL graphene with Coulomb interaction and a uniform gap by employing a renormalization group technique. Both configurations show rather different Coulomb physics which is mostly due to the different scaling of the energy in ML and BL. While in ML the Coulomb interaction always generates a gap in the electronic spectrum, which guarantees the finiteness of the Fermi velocity, in BL there is a proper metal-insulator transition, i. e. both gapped and gapless regime are possible. In the gapless regime of the BL the Coulomb interaction leads to the emergence of the linear relativistic spectrum.

We gratefully acknowledge useful discussions with S. Savel'ev, B. Dóra, and A. Sedrakyan. AS has been supported by the DPG-grant ZI 305/5-1.

-
- [1] D. C. Elias, et al., *Science* **323**, 610 (2009).
 - [2] O. Taisuke, et al., *Science* **18**, 951 (2006).
 - [3] K. Ziegler, *Phys. Rev. Lett.* **102**, 126802 (2009); *Phys. Rev. B* **79**, 195424 (2009).
 - [4] V. Juričić, et al., *Phys. Rev. B* **80**, 081405(R) (2009).
 - [5] D. T. Son, *Phys. Rev. B* **75**, 235423 (2007).
 - [6] E. G. Mishchenko, *Phys. Rev. Lett.* **98**, 216801 (2007); *Europhys. Lett.* **83**, 17005 (2008).
 - [7] D. E. Sheehy and J. Schmalian, *Phys. Rev. Lett.* **99**, 226803 (2007).
 - [8] A. H. Castro Neto, et al., *Rev. Mod. Phys.* **81**, 109 (2009).
 - [9] J.E. Drut and T.A. Lähde, *Phys. Rev. Lett.* **102**, 026802 (2009).
 - [10] T. Stauber, et al., *Phys. Rev. B* **71**, 041406(R) (2005).
 - [11] M. S. Foster and I. L. Aleiner, *Phys. Rev. B* **77**, 195413 (2008).
 - [12] I. F. Herbut, et al., *Phys. Rev. Lett.* **100**, 046403 (2008).
 - [13] F. Schuetz, et al., *Phys. Rev. B* **72**, 035107 (2005); F. Schuetz and P. Kopietz, *J. Phys. A* **39**, 8205 (2006).
 - [14] C. Wetterich, *Phys. Lett. B* **301**, 90 (1993).
 - [15] T. R. Morris, *Int. J. Mod. Phys. A* **9**, 2411 (1994).
 - [16] J. González, et al., *Phys. Rev. B* **59**, R2474 (1999).